

Supporting Material

Enhancing the anti-fouling and fouling removal properties of thin-film composite membranes through an intercalated functionalization method

Environmental Science: Water Research & Technology

Caihong Liu^{1,#,*}, Andreia F. Faria^{2,#}, Jennifer Jackson², Qiang He¹, Jun Ma³

¹ Key Laboratory of Eco-environments in Three Gorges Reservoir Region, Ministry of Education, College of Environment and Ecology, Chongqing University, Chongqing 400044, China

² Engineering School of Sustainable Infrastructure & Environment (ESSIE), Department of Environmental Engineering Sciences, University of Florida, Gainesville, FL 32611-6580, USA

³ State Key Laboratory of Urban Water Resource and Environment, Harbin Institute of Technology, Harbin, Heilongjiang 150090, China

[#]These authors contributed equally to this work.

*Corresponding Author

*E-mail: lchhit@126.com (C.L).

Number of Pages: 14

Number of Sections: 2

Number of Figures: 10

Section S1. Bacterial Morphology Characterization

The morphology of the attached *P. aeruginosa* cells on the pristine, PDA-PSBMA, and PDA-Ag-PSBMA TFC membranes was observed through SEM. After exposure to bacterial suspension, the membranes were rinsed with sterile PBS, and the attached cells were fixed using a Karnovsky's solution (2% paraformaldehyde and 2.5% glutaraldehyde diluted in 0.2 M Sorenson's buffer, pH 7.2) for 3 h. The cells deposited on membrane surface were consecutively dehydrated by water-ethanol (50:50, 30:70, 20:80, 10:90, and 100% ethanol) and ethanol-freon solutions (50:50, 25:75, and 100% freon) for 10 min each. After the sequential dehydration steps, the membrane coupons were dried overnight in a desiccator at room temperature. The samples were then sputter-coated with 10 nm of chromium (Denton Vacuum, Desk V) and imaged by SEM (Hitachi SU-70). The SEM images are shown in Figure S5.

Section S2. CLSM Imaging and Analysis Protocol

The stained membrane samples were placed on a custom-built chamber for CLSM imaging.^{1,2} A CLSM microscopy (Zeiss LSM 510, Carl Zeiss, Inc.) equipped with a plan-apochromat was used to capture confocal images of the biofilm. SYTO 9, PI, and Con A were excited with 488 nm argon, 561 nm diode-pumped solid state, and 633 nm helium-neon laser, respectively. At least six Z stack random fields ($635\ \mu\text{m} \times 635\ \mu\text{m}$) with a slice thickness of $2.14\ \mu\text{m}$ were collected from each sample to obtain a representative 3D biofilm image. At least eight smaller stack regions ($90\ \mu\text{m} \times 90\ \mu\text{m}$) with a slice thickness of $1.2\ \mu\text{m}$ were captured for biofilm dimension calculation. Confocal images were analyzed using Auto-PHLIP-ML, Image-J, and MATLAB software, as suggested by previous publications.¹⁻⁴ Biovolume and thickness were determined for the live cells, dead cells, and EPS of the biofilm for all the samples. Average biofilm thickness was calculated by averaging the thickness of these three components.

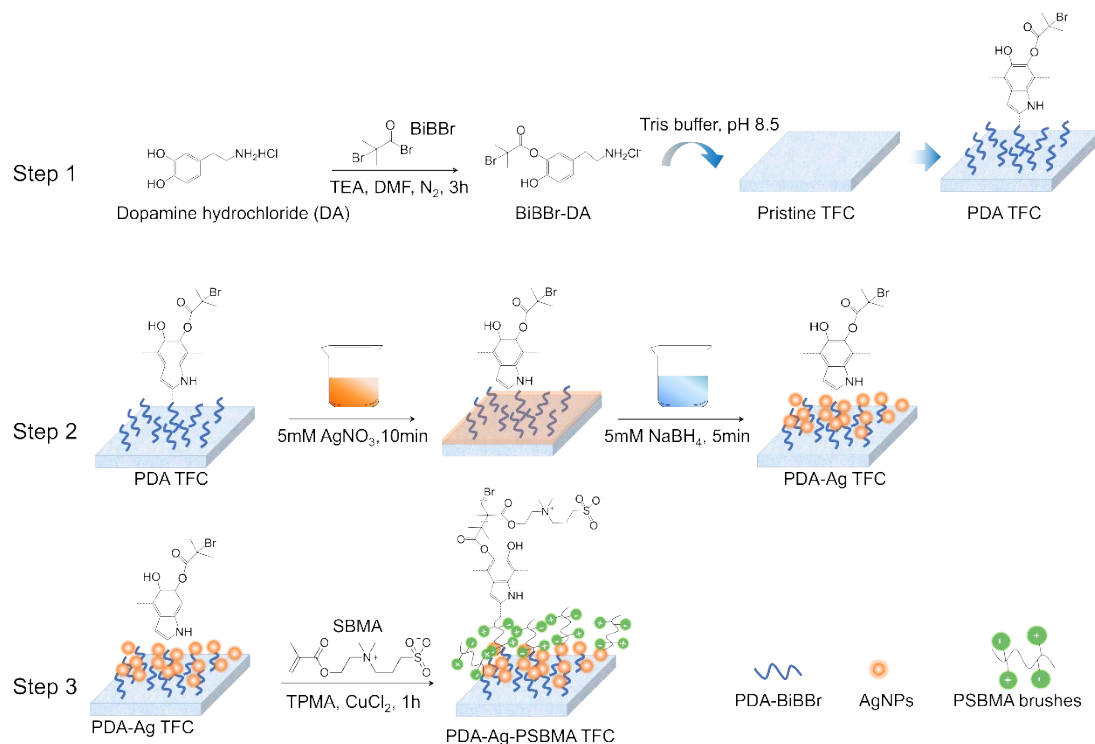


Fig.S1. Schematic illustration of the intercalated functionalization strategy. Step 1: polydopamine (PDA) coupled with initiator BiBBr is immobilized on the membrane surface by reacting dopamine chloride with the initiator BiBBr and further self-polymerization of dopamine (PDA TFC membrane). Step 2: intercalation with AgNPs is enabled through the reaction of coated Ag⁺ ions with NaBH₄ (PDA-Ag TFC membrane). Step 3: PSBMA polymer brushes are grafted on the PDA-Ag TFC membranes via ATRP method (PDA-Ag-PSBMA TFC membrane).

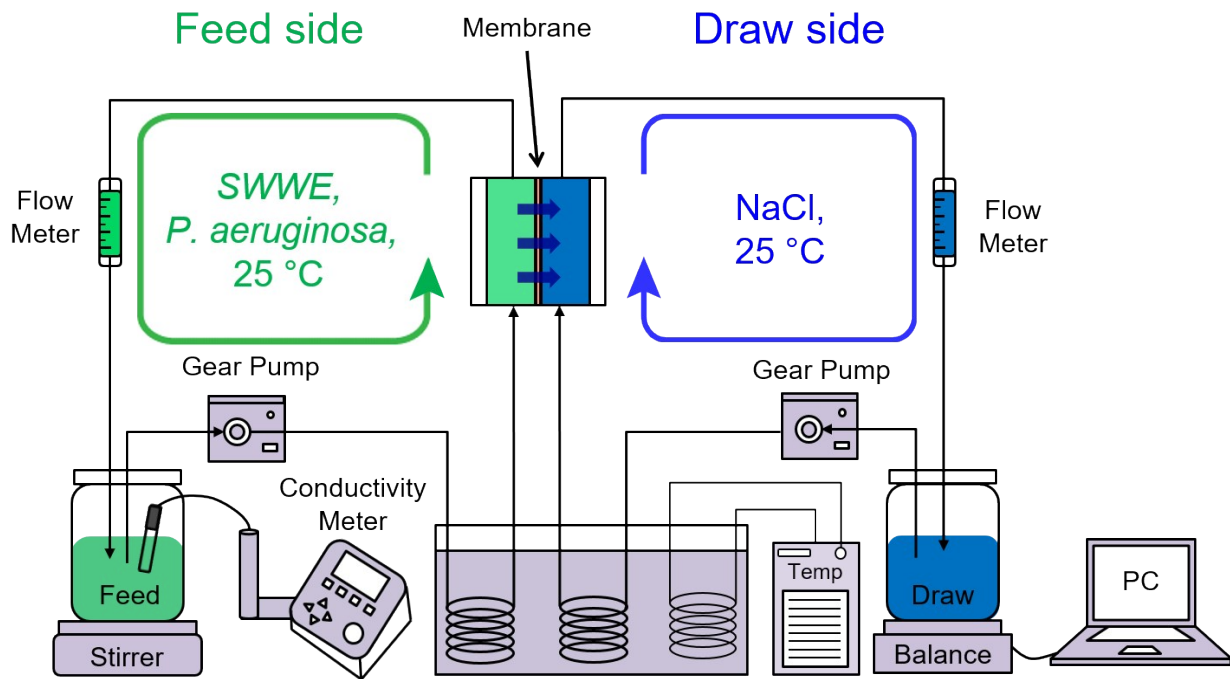


Fig.S2. Illustration of the FO membrane setup for dynamic biofouling experiments.

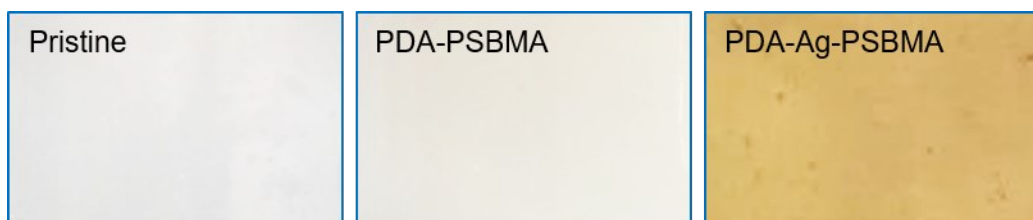


Fig.S3. Digital photographs of the pristine, PDA-PSBMA and PDA-Ag-PSBMA TFC membranes.

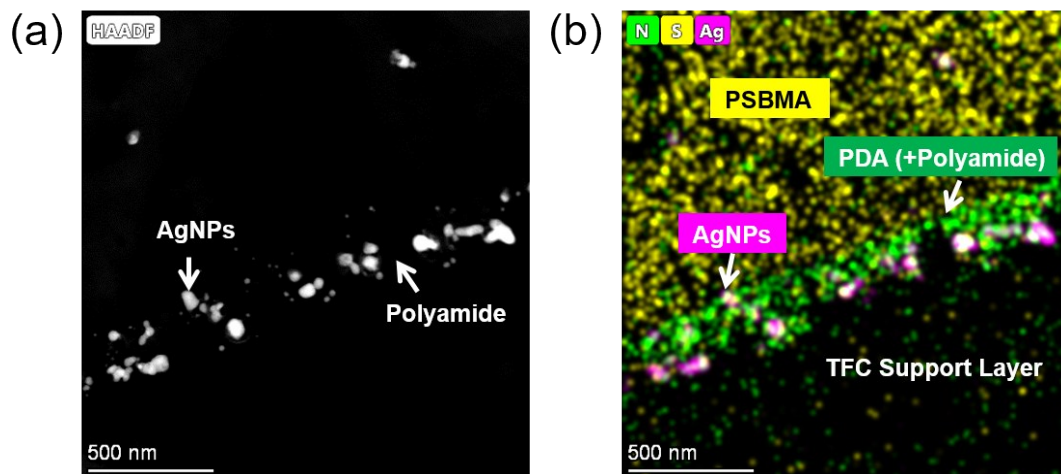


Fig.S4. (a) Cross-section dark-field TEM image and (b) STEM-EDX elemental mapping of the PDA-Ag-PSBMA membrane. In the STEM-EDX mapping image, magenta, green, and yellow colors denote AgNPs, nitrogen (N), and sulfur (S), respectively.

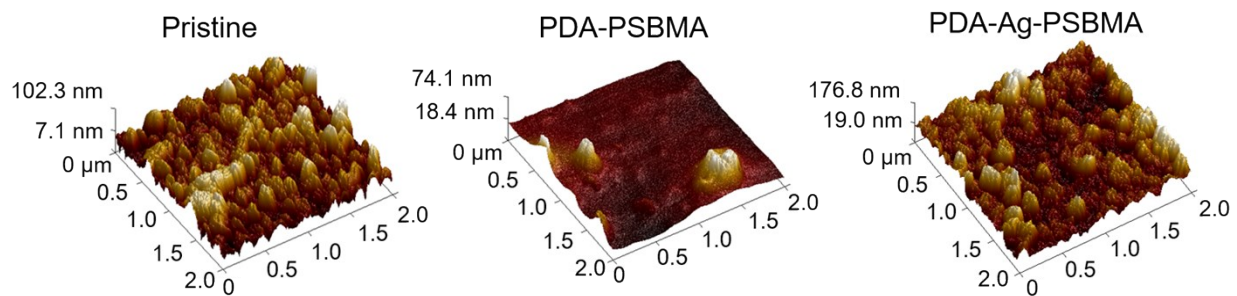


Fig.S5. AFM 3D images of pristine, modified PDA-PSBMA TFC, and PDA-Ag-PSBMA TFC membranes.

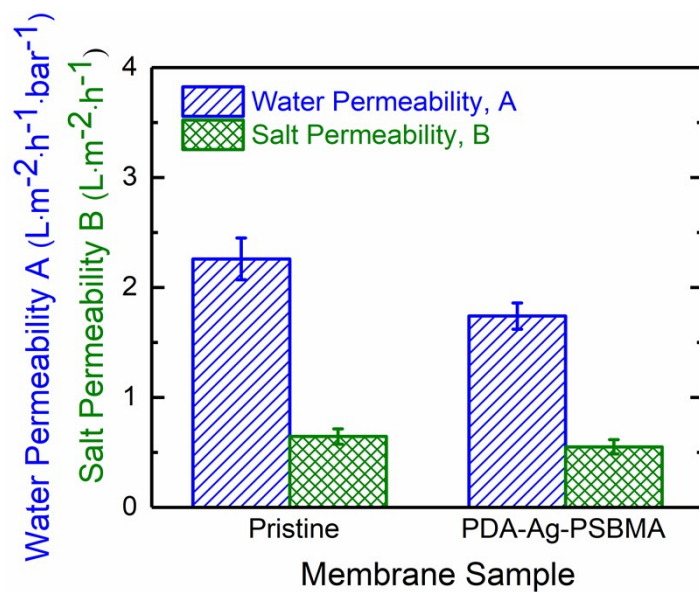


Fig.S6. Water permeability coefficient (*A*), and salt permeability coefficient (*B*), for pristine and modified PDA-Ag-PSBMA TFC membranes. These transport parameters were calculated from the FO four-step characterization method.⁵



Fig.S7. (A) LB plates after inoculation and growth of *P. aeruginosa* cells that were attached to the pristine, PDA-PSBMA, and PDA-Ag-PSBMA TFC membranes. (B) SEM images displaying the morphological characteristics of *P. aeruginosa* cells on the surface of pristine, PDA-PSBMA, and PDA-Ag-PSBMA TFC membranes after exposure for 3 h.

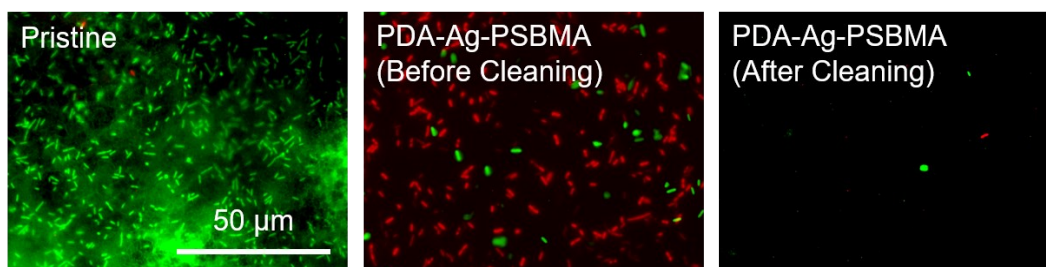


Fig.S8. Representative epifluorescence images of live (green) and dead (red) *P. aeruginosa* cells on the surface of pristine, and PDA-Ag-PSBMA membranes (before and after cleaning at 250 rpm for 1 h).

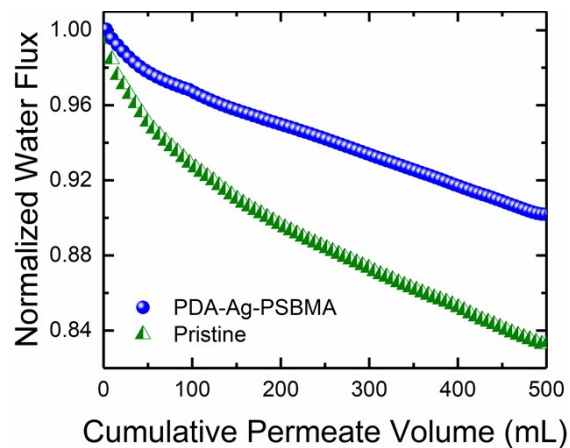


Fig.S9. Normalized water flux for pristine and modified PDA-Ag-PSBMA TFC membranes during the biofouling run. The initial ionic strength, electric conductivity, and pH of the synthetic feed solution were 15.9 mM, $1142 \pm 50 \mu\text{S}$, and 7.6 ± 0.2 , respectively. The initial water flux was $20 \text{ L} \cdot \text{m}^{-2} \cdot \text{h}^{-1}$, and temperature was maintained at $25.0 \pm 0.5 \text{ }^\circ\text{C}$.

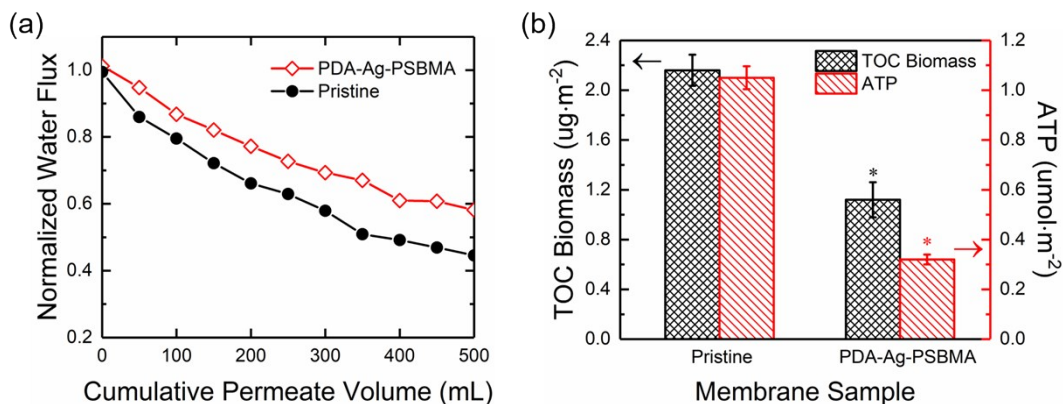


Fig.S10. (a) Normalized water flux of pristine and modified PDA-Ag-PSBMA TFC membranes due to fouling by sewage wastewater collected from the wastewater treatment facility at the Chongqing University campus. (b) Deposited TOC biomass and metabolic (ATP assay) in the biofilm after fouling runs. Before dynamic fouling experiments, the raw wastewater was prefiltered through a 10 mm cartridge filter. Results were acquired from three independent duplicates. Asterisks indicate that the TOC biomass and ATP accumulated on the modified membranes showed a statistically significant difference compared to those on the pristine TFC membranes ($p < 0.05$).

REFERENCES:

1. Kwan, S. E.; Bar-Zeev, E.; Elimelech, M., Biofouling in forward osmosis and reverse osmosis: Measurements and mechanisms. *Journal of Membrane Science* **2015**, *493*, 703-708.
2. Bar-Zeev, E.; Perreault, F.; Straub, A. P.; Elimelech, M., Impaired Performance of Pressure-Retarded Osmosis due to Irreversible Biofouling. *Environmental science & technology* **2015**, *49*, (21), 13050-13058.
3. Xie, M.; Lee, J.; Nghiem, L. D.; Elimelech, M., Role of pressure in organic fouling in forward osmosis and reverse osmosis. *Journal of Membrane Science* **2015**, *493*, 748-754.
4. Xie, M.; Bar-Zeev, E.; Hashmi, S. M.; Nghiem, L. D.; Elimelech, M., Role of Reverse Divalent Cation Diffusion in Forward Osmosis Biofouling. *Environmental science & technology* **2015**, *49*, (22), 13222-13229.
5. Tiraferri, A.; Yip, N. Y.; Straub, A. P.; Romero-Vargas Castrillon, S.; Elimelech, M., A method for the simultaneous determination of transport and structural parameters of forward osmosis membranes. *Journal of Membrane Science* **2013**, *444*, 523-538.